

## Present status of lattice QCD at nonzero $T$ and $\mu$

RAJIV V GAVAI

Department of Theoretical Physics, Tata Institute of Fundamental Research,  
Mumbai 400 005, India  
E-mail: gavai@tifr.res.in

**Abstract.** I review a few selected topics in lattice quantum chromodynamics, focusing more on the recent results. These include (i) the equation of state and speed of sound, (ii)  $J/\psi$  suppression, (iii) flavour correlations and (iv) the QCD phase diagram in the  $\mu$ - $T$  plane.

**Keywords.** Lattice; quantum chromodynamics; quark-gluon plasma; flavour correlations.

**PACS Nos** 11.15.Ha; 12.38.Mh

### 1. Introduction

In the continuous quest for quark-gluon plasma (QGP), which began about two decades ago at the SPS at CERN, Geneva, and has continued in a spectacular way at the Relativistic Heavy Ion Collider (RHIC) at BNL, New York, USA, one now has a plethora of theoretical suggestions for signals of QGP as well as huge amounts of data. The Large Hadron Collider (LHC) at CERN will take us to even higher colliding energies of heavy ions than before. In the complex task of putting the pieces of the jigsaw puzzle together to establish eventually this new phase of strongly interacting matter from the experimental data, one needs as much of theoretical help as can be provided. In particular, theory needs to provide reliable estimates of various quantities, such as the transition temperature, the equation of state (EoS) and the critical energy density needed to reach the QGP phase. Information on various properties of QGP, such as, the nature of its excitations and the strength of their interactions would also be crucial in the experimental search.

Quantum chromodynamics (QCD) defined on a space-time lattice, lattice QCD, is the only successful and reliable tool to extract the desired non-perturbative physics from the underlying theory. This first-principles based and (essentially) parameter-free approach should be contrasted with the results from other approaches, primarily models. Thus not only does lattice QCD lead us to the phenomenon of quark confinement and spontaneous breaking of chiral symmetry (or

the answer to why pion is so light) but it also provides us with a quantitative understanding of the spectrum of hadrons and their other properties. Indeed, these results have been accorded an ‘iconic’ status in theoretical high energy physics recently [1]. One hopes that similar reliable information on the transition to QGP and properties of QGP will be provided by these techniques, and any experimental demonstration of a failure of a prediction of lattice QCD, such as the transition to quark-gluon plasma, will be tantamount to one of the best experimental evidence for physics beyond the standard model, discussed rather extensively at this workshop.

Lattice formulation of QCD associates quark fields,  $\psi(x)$ , and the antiquark fields  $\bar{\psi}(x)$  with the site  $x = (x_1, x_2, x_3, x_4)$  of a four-dimensional hypercubic lattice. The (inverse) lattice spacing  $a$  acts as the ultra-violet cut-off. Continuum limit of vanishing  $a$  corresponds to removal of the cut-off. As in the case of the continuum field theory, one obtains a lattice gauge theory by demanding invariance of the Lagrangian for free quark–antiquarks (e.g. obtained by a straightforward discretization of the usual Dirac Lagrangian) under any *local* phase rotation of these fields. This can be accomplished by introducing lattice gauge fields  $U_x^\mu \equiv U_\mu(x)$  which are associated with a directed link from the site  $x$  to  $x + \hat{\mu}a$ .

Defining a partition function  $\mathcal{Z}$  for these fields, akin to a complicated version of the familiar Ising model partition function

$$\begin{aligned} \mathcal{Z} &= \int \prod_{x, \hat{\mu}} dU_\mu(x) \prod_x d\psi(x) d\bar{\psi}(x) e^{-S_G - S_F} \\ &= \int \prod_{x, \hat{\mu}} \prod_f \det M(am_f^{\text{sea}}, a\mu_f) e^{-S_G}, \end{aligned} \quad (1)$$

where  $S_G$  and  $S_F$  are gluonic and quark actions,  $M$  is the Dirac matrix in  $x$ , colour, spin, flavour space for fermions of mass  $am_f^{\text{sea}}$  and  $a\mu_f$  is the chemical potential (in lattice units). One can compute quantum expectation values of any physical observable  $\Theta$ , which may contain fermion propagators of mass  $am^{\text{valence}}$ , as averages with respect to the  $\mathcal{Z}$  above. Thus, e.g., masses of physical particles are obtained from the exponential decays of appropriate correlation functions. Of relevance to heavy-ion physics, is the investigation of eq. (1) at finite temperature, which is achieved by taking a  $N_s^3 \times N_t$  lattice, where  $N_s$  is the number of lattice sites in a space direction and  $N_t$  in the time direction. This leads to volume  $V = N_s^3 \cdot a^3$  and temperature  $T = (aN_t)^{-1}$ . Clearly, one needs to have  $N_s \gg N_t$ .

The Monte Carlo technique to evaluate the expectation value of any physical observable, consists of the following three steps: (1) Generate as large an ensemble of sets of links  $\{U_x^\mu\}$  for the whole lattice as possible, such that each set of  $\{U_x^\mu\}$  occurs with a probability proportional to  $\prod_f \det M_f \cdot \exp[-S_G(\{U_x^\mu\})]$ , (2) evaluate the observable for each configuration  $\{U_x^\mu\}$  and (3) take its average over all the configurations in the set. Due to the enormity of the computational task to generate the set of  $\{U_x^\mu\}$  for full QCD, i.e., for a theory with all virtual quark loops included, one employs increasingly severe approximations with decreasing amount of computer time. These are (i) full QCD simulations on smaller lattices, (ii) partially quenched QCD simulations with  $am^{\text{sea}}$  large and greater than  $am^{\text{valence}}$  and (iii) quenched QCD simulations with  $am^{\text{sea}} = \infty$  (i.e. no dynamical quarks). The

early lattice results and today's best results are obtained in the quenched approximation. However, some aspects, such as the order of the phase transition, do depend strongly on the dynamical quark content, necessitating a judicious use of the quenched approximation.

A transition temperature of  $T_c \sim 170$  MeV for two-flavour QCD has been earlier estimated [2,3]. The transition seems to be continuous. For three light flavours, the transition temperature seems to be lower by about 20 MeV [3], bracketing our world of two light and one heavy flavours, by that amount. Similarly, equation of state (EoS) has been predicted by lattice QCD. Other quantities, notably the Wróblewski parameter  $\lambda_s$ , which measures the strangeness enhancement in heavy-ion physics, have also been predicted [4] by lattice QCD. These earlier results were obtained either in quenched approximation or on coarser  $N_t = 4$  lattices for full theory. Thrust of the new results in the recent past has been on (i) employing larger lattices to achieve continuum limit and to lighter quarks, (ii) more complex observables, such as speed of sound, transport coefficients, fluctuations and susceptibilities,  $J/\psi$ -dissolution/persistence, dileptons etc. and (iii) theoretically more challenging  $T$ - $\mu$  phase diagram. An interesting comparison of predictions of conformally invariant QCD-like theories with lattice results has also been made.

For reasons of both time and interest, I have chosen to limit this review to a few of the above-mentioned selected topics. A quick overview of the basic lattice gauge theory can be found in [5] or many textbooks. In the next sections, I intend to discuss only the recent results, leaving out many technical details. A short summary is provided at the end. Let me emphasise here that one has witnessed recently a lot of activity in model building to explain the lattice QCD results. These include quasiparticle models, hadron resonance gas, quarkonia from lattice  $Q\bar{Q}$  potential, sQGP and coloured states. Many of them can, and eventually did, form interesting topics for working group discussions, leading even to a paper on the archive eventually.

## 2. Properties of QGP

In this section I shall review the recent progress made in the past few years in pinning down various properties of QGP using the lattice approach. These have been chosen for their direct connection with the experimental heavy-ion physics.

### 2.1 Equation of state and speed of sound

Equation of state plays a critical role in a variety of aspects of heavy-ion collisions. Thus estimates of the energy density at  $T_c$  are required to choose the appropriate heavy-ion colliding energy. Recently results for the pressure and energy density for  $N_t = 6$  lattices at nonzero temperature QCD with 2+1 flavours of improved staggered quarks were reported [6]. Using improved gauge action and improved staggered quark action to eliminate the cut-off effects at  $\mathcal{O}(a^2)$  and with the heavy quark mass  $m_s$  fixed at approximately the physical strange quark mass but with the two degenerate light quark masses  $m_{ud} = 0.1m_s$  or  $0.2m_s$ , it was found that

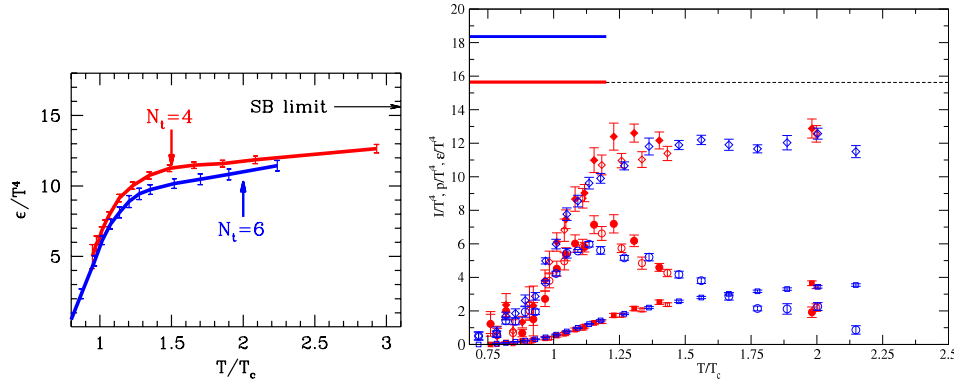


**Figure 1.** Recent results for EoS on  $N_t = 6$  lattices from refs [7] (left) and [6] (right).

the results were in agreement with those on  $N_t = 4$  lattices, as seen on the right panel of figure 1.

Using another improved action, similar results were obtained by another group [7] for quark masses corresponding to physical meson masses. These are displayed in the left panel of figure 1. Again, one sees small changes compared to the  $N_t = 4$  case. In particular, the critical energy density,  $\epsilon(T_c)$  is  $\sim 6T_c^4$  still. One note of caution though is that the spatial volumes in physical units (such as inverse pion mass) are rather small and some changes may therefore be expected in true thermodynamic limit.

Velocity of sound,  $C_s$ , in QGP and dense hadronic media is a crucial input to many phenomenological studies based on the hydrodynamical approach. The presence of elliptic flow was established in this way and has been regarded as a key evidence in favour of the collective behaviour of the produced matter. Estimates of  $C_s$  in the transition region have recently been obtained using a new approach [8] which relates it to the temperature derivative of the anomaly measure  $\Delta/\epsilon$ , where  $\Delta = \epsilon - 3P$ . Combining further with a new method to obtain  $\epsilon$  and  $P$  by an improved operator method, which leads to positive pressure on all lattices at all temperatures,  $C_s$  as well as the specific heat  $C_v$  were obtained [9] in the continuum limit.

Lattices with large temporal extent,  $N_t = 8, 10$  and  $12$ , and spatial sizes up to  $N_s = 38$  were used in the quenched approximation to obtain the results shown in figure 2. One sees in the left panel that  $C_v \sim 4\epsilon$  for  $T \geq 2T_c$  but its value is not close to the ideal gas limit. On the other hand, the speed of sound shown on the right,  $C_s^2$ , is close to the ideal gas limit by  $2T_c$ . Interestingly, it does not seem to show any structure near  $T_c$ , whereas the specific heat does hint at a peak at  $T_c$ . It has been argued that fluctuations in  $p_T$  may be able to unravel the specific heat and its peak from heavy ion data. More theoretical studies are needed to sharpen this idea and to obtain a precise experimental measure. The above lattice results are encouraging for such studies.

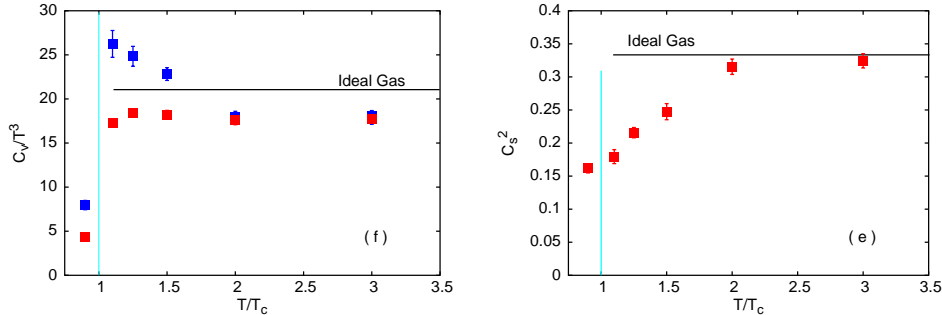


**Figure 2.**  $C_v/T^3$  and  $4\epsilon/T^4$  (left) and  $C_s^2$  (right) as a function of  $T/T_c$  for quenched QCD in continuum from ref. [9].

An exciting and curious agreement of the entropy density  $s$  computed for quenched continuum QCD has been reported [9] recently with that obtained using strong coupling prediction in the supersymmetric Yang–Mills theory in the temperature range of  $2\text{--}3T_c$ . The latter predicts [10]  $s/s_0 = f(g^2 N_c)$ , where  $f(x) = \frac{3}{4} + \frac{45}{32}\zeta(3)x^{-3/2} + \dots$  and  $s_0 = \frac{2}{3}\pi^2 N_c^2 T^3$  is the ideal gas entropy density. In contrast,  $s_0 = \frac{4}{45}\pi^2(N_c^2 - 1)T^3$  for quenched QCD (i.e., without supersymmetry). Nevertheless, the prediction does seem to do well both in normalization and the shape in spite of the badly broken supersymmetry for the lattice results. Understanding this and extending it to even lower temperatures where weak coupling methods do fail would be very exciting indeed.

## 2.2 QGP – (almost) perfect liquid?

From the measured azimuthal angle distribution of various particles produced in a collision, one extracts a quantity called elliptic flow,  $v_2$ . Phenomenological studies of  $v_2(p_T)$  show it to be consistent with QGP displaying ideal hydrodynamical behaviour [11]. Indeed, from the small deviations, one can derive [12] a bound on the shear viscosity,  $\eta$ , of QGP:  $\Gamma_s/\tau_0 = \frac{4}{3}\eta/sT\tau_0 \leq 0.1$ , where  $\tau_0$  is the formation time. This suggests a very small value for the dimensionless ratio,  $\eta/s$ , whereas perturbation theory leads to a large value for it, giving rise to the description of QGP produced at RHIC as being an almost perfect and strongly coupled liquid.

Kubo’s linear response theory permits the determination of the transport coefficients, such as  $\eta$ , in terms of equilibrium correlation functions. In particular, one needs the correlation function of the energy–momentum tensor. This is obtained on lattices in  $x$ -space and transformed to the momentum space, i.e. obtained at discrete Matsubara frequencies. In order to extract the transport coefficients, which are determined by the behaviour of the retarded correlation functions at small frequencies  $\omega$ , one continues these in the complex  $\omega$ -plane. Figure 3 displays the latest results [13] on the desired ratio  $\eta/s$  on lattices as large as  $24^3 \times 8$  but in QCD without dynamical quarks. Also shown are the estimates from perturbation

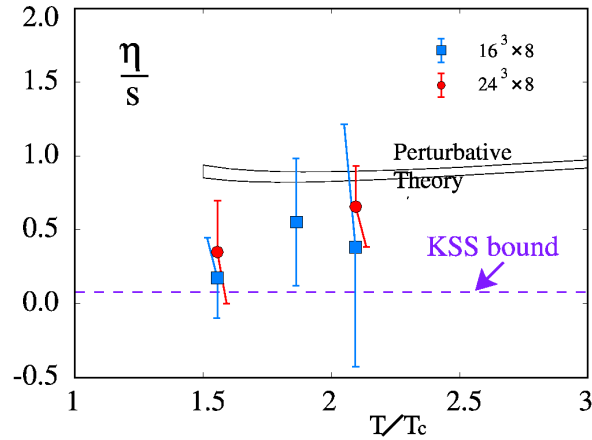


**Figure 3.** Ratio of shear viscosity and entropy density for quenched QCD [13].

theory and an analytic bound from supersymmetric QCD which is fairly close to the bound from hydrodynamics quoted above. The lattice results start from being close to these bounds in the vicinity of the transition and show a tendency of going towards the larger perturbative value as temperature increases. Calculations on larger lattices and with inclusion of dynamical quarks are needed to confirm these results and to make them more precise. Nevertheless their proximity to the bound from the heavy-ion data is very encouraging.

### 2.3 Anomalous $J/\psi$ suppression

Suppression of the most famous quarkonium,  $J/\psi$ , has been widely known as a signal for QGP production in heavy-ion collisions and a lot has been learnt [14] since the early data on this subject. Recently, the NA50 Collaboration from CERN came out with their precise results. Moreover,  $J/\psi$  suppression has been observed at the RHIC in BNL as well. A brief summary of these latest results [15] from CERN and BNL and their comparison with model predictions are given below:

- Sulphur–uranium and peripheral lead–lead (Pb–Pb) results for the ratio of  $J/\psi$  production cross-section to that of Drell–Yan behave as expected from extrapolations of proton–nucleus data. Glauber model with an absorption cross-section of  $4.18 \pm 0.35$  mb for the  $J/\psi$ , determined from  $p$ -A data, decided these expectations.
- Pb–Pb central data on the other hand, show anomalous suppression with respect to the corresponding expectations.
- The  $\psi'/\text{DY}$  ratio is *not* compatible for even S–U and peripheral Pb–Pb with similar expectations from proton–nucleus (with an absorption cross-section of  $7.6 \pm 1.12$  mb).
- Thus,  $\psi'$  anomalous suppression sets in earlier than  $J/\psi$ .

- Theoretical models that were successful in describing the above SPS, CERN data predicted too much suppression at RHIC compared to what was observed by PHENIX at RHIC.

The impressive sets of data from CERN and RHIC have attracted a lot of attention from lattice experts. The original Matsui–Satz idea of  $J/\psi$  suppression was based on simple quarkonium potential models and an ansatz for the temperature dependence of the potential. It seems very important to check whether similar conclusions follow from the underlying theory, QCD, with as few assumptions as possible. Recognition of the so-called MEM (maximum entropy method) as a tool to extract the spectral functions of mesons from the temporal correlators computed on the lattice has permitted a fresh assessment of the original idea. Figure 4 exhibits the spectral functions [16] of the  $\eta_c$ ,  $J/\psi$  and the  $\chi$  states in quenched QCD at various temperatures.

As seen on the right panel, the peaks for  $\chi_c$  do not show any significance beyond the error bars by  $1.1T_c$ , i.e. they do seem to dissolve in agreement with the potential model estimate but the left panel shows persistence of  $J/\psi$  and  $\eta_c$  up to  $2.25T_c$ ; they seem to melt away only by  $3T_c$ . Similar results have been obtained by other groups [17], although differences persist on the precise melting temperature for  $J/\psi$ . In addition to the need to iron them out, by requiring larger lattices, uniform criteria and a comparison at the correlator levels, one has to also include dynamical quarks in these computations in quenched QCD. There is a lot more work to do but one can still ask whether these results should lead to changes in expectations of the suppression patterns as a function of temperature or the colliding energy since only a fifth to a third of the observed  $J/\psi$  come from the states which do melt soon after the transition. Another interesting question is about quarkonia moving in the heat bath. One may expect them to see more energetic gluons, leading to more dissociation at the same temperature as the momentum increases. Preliminary results [18] show this to be indeed true for even  $J/\psi$  and  $\eta_c$ . However, the effect seems significant both below and above the transition, leading one to wonder whether it plays any role in the anomalous suppression seen in the heavy-ion collisions.

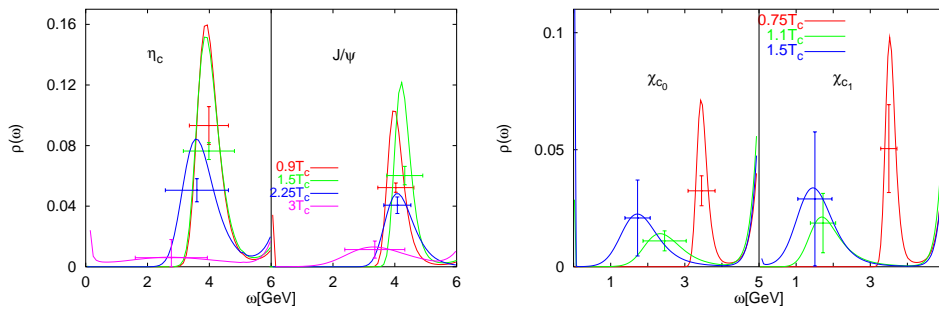


**Figure 4.** Spectral functions of  $\eta_c$ ,  $J/\psi$  (left) and the  $\chi$  states (right) in quenched QCD [16] at various temperatures indicated.

### 3. QCD phase diagram

Lattice QCD at nonzero baryon density may help us in understanding, or even deriving, an interesting physical phenomena, namely, color superconductivity, which may find applications in the astrophysics of strange quark stars. From a theoretical viewpoint, it is, of course, crucial in completing the  $\mu_B$ - $T$  phase diagram of QCD. Both the numerical and the analytical methods used at finite temperature are inadequate in this case due to the fact that the fermionic determinant  $\det M(\mu)$  is complex for  $\mu \neq 0$ , commonly referred to as the sign (or the phase) problem. Various models, notably the Nambu–Jona–Lasinio and the random matrix model, have played a big role in shaping our understanding of the QCD phase diagram. However, there have been some new exciting developments in the recent past for small  $\mu$ . Most earlier attempts comprised of exploring first the zero temperature axis, where the problem is hardest. Recognizing this the latest strategy has been to work for small  $\mu$  in the vicinity of the quark–hadron transition, and study its behaviour as  $\mu$  is turned on. Various methods [19,20], such as the re-weighting method, a Taylor expansion in  $\mu$ , analytic continuation from imaginary  $\mu$ , have led to similar qualitative results. I will provide a flavour of these results by briefly mentioning here our results obtained by Taylor expansion, referring the reader to the original works in [19,20] for a detailed comparison.

The Taylor expansion method has several advantages over the others. Prime amongst them is the ease of taking continuum and thermodynamic limit. As mentioned in the Introduction, one *has* to take these limits for the results to have any relevance to the real world of experiments. The re-weighting method, for example, has a factor that grows exponentially with lattice size and also has no systematic control over discretization errors. Analytic continuation to real  $\mu$  is also done term by term in a small  $\mu$ -expansion. Employing the Taylor expansion, we [21] studied volume dependence at several  $T$  to (i) bracket the critical region and then to (ii) track its change as a function of volume. A strong volume dependence was found which changed the critical point obtained earlier by other methods substantially. The lattices we used were  $4 \times N_s^3$ , with  $N_s = 8, 10, 12, 16, 24$ , enabling us to vary the volume  $V = N_s^3 a^3$  at fixed temperature, i.e. fixed  $a$ . Our dynamical simulations for staggered fermions with two light dynamical ( $N_f = 2$  of mass  $m/T_c = 0.1$ ) quarks were made using the well-known  $R$ -algorithm with a trajectory length scaled  $\propto N_s$ . From [22], it is known that the transition temperature is  $T_c/m_\rho = 0.186 \pm 0.006$  and the choice of our quark mass corresponds to  $m_\pi/m_\rho = 0.31 \pm 0.01$ . While it is still high compared to the real world, it is one of the smallest pion mass so far used; lowering pion mass further necessitates even larger volumes than we were able to employ. Our simulations were made at  $T/T_c = 0.75(2), 0.80(2), 0.85(1), 0.90(1), 0.95(1), 0.975(10), 1.00(1), 1.045(1), 1.15(1), 1.25(2), 1.65(6)$  and  $2.15(10)$ . Typical statistics used was 50–100 in (max) autocorrelation units.

Defining  $\mu_f$  as the chemical potential for a flavour  $f = u, d, s$  and  $\mu_0 = \mu_u + \mu_d + \mu_s$  and  $\mu_3 = \mu_u - \mu_d$  as baryon and isospin chemical potentials, the respective density and susceptibility can be obtained from eq. (1) as

$$n_i = \frac{T}{V} \frac{\partial \ln \mathcal{Z}}{\partial \mu_i}, \quad \chi_{ij} = \frac{T}{V} \frac{\partial^2 \ln \mathcal{Z}}{\partial \mu_i \partial \mu_j}. \quad (2)$$

Setting  $\mu_f = 0$  after taking the derivatives,  $n_f = 0$  but  $\chi_{ij}$  are nontrivial. The diagonal  $\chi$ 's are found [23] to be

$$\chi_0 = \frac{1}{2} \left[ \mathcal{O}_1(m_u) + \frac{1}{2} \mathcal{O}_2(m_u) \right], \quad (3)$$

$$\chi_3 = \frac{1}{2} \mathcal{O}_1(m_u), \quad (4)$$

$$\chi_s = \frac{1}{4} \left[ \mathcal{O}_1(m_s) + \frac{1}{4} \mathcal{O}_2(m_s) \right]. \quad (5)$$

Here  $\mathcal{O}_i$  are traces of products of  $M^{-1}$ ,  $M'$  and  $M''$  and are estimated by a stochastic method:  $\text{Tr } A = \sum_{i=1}^{N_v} R_i^\dagger A R_i / 2N_v$ , and  $(\text{Tr } A)^2 = 2 \sum_{i>j=1}^L (\text{Tr } A)_i (\text{Tr } A)_j / L(L-1)$ , where  $R_i$  is a complex vector from a set of  $N_v$ , subdivided in  $L$  independent sets. Further details can be found in [21,23].

Denoting higher order susceptibilities by  $\chi_{n_u, n_d}$ , the pressure  $P$  has the expansion in  $\mu$ :

$$\frac{\Delta P}{T^4} \equiv \frac{P(\mu, T)}{T^4} - \frac{P(0, T)}{T^4} = \sum_{n_u, n_d} \chi_{n_u, n_d} \frac{1}{n_u!} \left( \frac{\mu_u}{T} \right)^{n_u} \frac{1}{n_d!} \left( \frac{\mu_d}{T} \right)^{n_d}. \quad (6)$$

From this expansion, a series for baryonic susceptibility can be constructed. Its radius of convergence gives the nearest critical point. Successive estimates for the radius of convergence can be obtained from these terms using  $r_n = \sqrt{|\chi_B^n / \chi_B^{n+2}|}$  or  $\rho_n = [|\chi_B^0 / \chi_B^n|]^{1/n}$ . We used terms up to 8th order in  $\mu$ , i.e., estimates from 2/4, 4/6 and 6/8 terms of the series eq. (6).

The ratio  $\chi_{11} / \chi_{20}$  can be shown [21] to yield the ratio of widths of the measure in the imaginary and real directions at  $\mu = 0$ . This argument for the measure of the imaginary part of the fermionic determinant can be generalized to nonzero  $\mu$  with some care, by constructing similarly as above the coefficients for the off-diagonal susceptibility,  $\chi_{11}(\mu)$ .

Before going on further to the results on the critical point, let us take a detour of interest to the current heavy-ion experiments. Quark number susceptibilities (QNS) which contribute the first nontrivial term in the above Taylor expansion also have their own independent physical and theoretical relevance. They are crucial for some signatures of quark-gluon plasma such as fluctuations of charge and/or baryon number, and production of strangeness. Their additional theoretical importance is due to the check they provide on resummed perturbation expansions or any other scenario for the high  $T$  phase.

### 3.1 The Wróblewski parameter and baryon-strangeness correlation

Here we will touch upon two different aspects of the physics hidden in the QNS. Ideally, one needs to obtain QNS in the continuum limit to extract any quantity

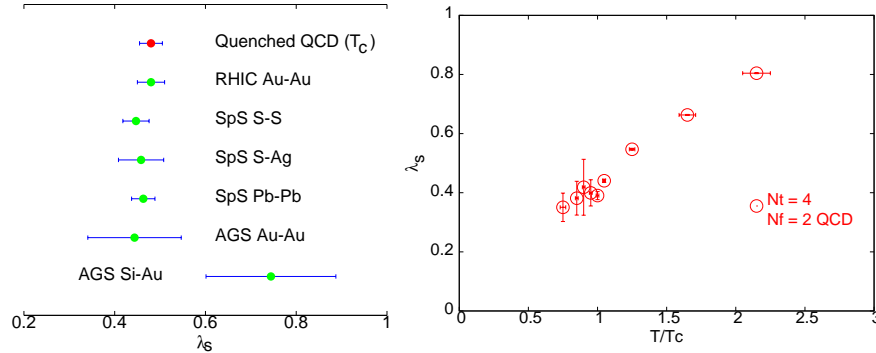


**Figure 5.** Comparison of lattice results on the Wróblewski parameter for quenched QCD with results from CERN and BNL (left). Corresponding full QCD results as a function of  $T/T_c$  (right). Taken from refs [4,24] respectively.

of interest for heavy-ion collisions. It has recently been shown that one can construct [24] robust ratios which have negligibly small theoretical and experimental systematic error. The primary amongst them is the Wróblewski parameter. Defined as the ratio of the strange particles and the non strange particles produced in a collision, it has been studied widely as a measure of the strangeness production. Interestingly, most heavy-ion collision data seem to yield a factor two higher value for it than other hadronic collisions. Using the continuum values for QNS, and under certain assumptions [4], one obtains  $\lambda_s(T_c) = 2\chi_s/(\chi_u + \chi_d) \approx 0.4-0.5$  which compares remarkably well with its latest RHIC value  $0.47 \pm 0.4$ , as shown in the left panel of figure 5. While these results were obtained in quenched QCD in the continuum limit, also the full QCD results [24] shown in the right panel but on a small temporal lattice ( $N_t = 4$ ) are in very good agreement with these, as expected of a robust ratio.

QNS can also be put to use in studying the correlation between quantum numbers  $K$  and  $L$  through the ratio  $C_{(KL)/L} = \frac{\langle KL \rangle - \langle K \rangle \langle L \rangle}{\langle L^2 \rangle - \langle L \rangle^2} \equiv \frac{\chi_{KL}}{\chi_L}$ . Again being ratios, these too are expected to be theoretically and experimentally robust. Such a strangeness-baryon number correlation,  $C_{BS} = -3(\chi_{BS}/\chi_S)$ , was proposed [25] as a distinguishing test between the various models/pictures of quark-gluon plasma near  $T_c$ . This, or the similarly defined strangeness-electric charge correlation,  $C_{QS}$ , is expected to be unity if quarks are the sole carriers of these quantum numbers (others being very heavy). On the other hand, the so-called sQGP model of Shuryak-Zahed [26] predicts these to be 0.66 and 1.2 respectively. Our lattice results [24] are exhibited in figure 6.

While one sees very different values for both  $C_{BS}$  and  $C_{QS}$  below  $T_c$ , their rapid approach to unity clearly indicates the presence of quark-like degrees of freedom immediately above  $T_c$ . In particular, the object which carries unit strangeness also has a baryon number of  $-1/3$  and a charge of  $1/3$ , just like a strange antiquark would. We have found that a variation of the strange quark mass,  $m_s/T_c$ , between 0.1 and 1.0 does not alter either the value for  $T \geq T_c$ , or its  $T$ -independence. A natural explanation of the  $T$ -behaviour arises if strange excitations with baryon number become lighter at  $T_c$ .  $T$ -independence further suggests existence of a single

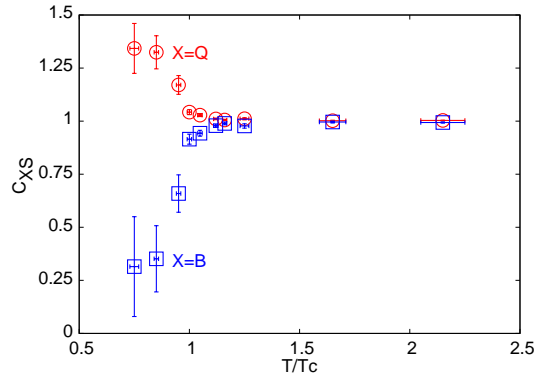


**Figure 6.**  $C_{BS}$  and  $C_{QS}$  as functions of  $T/T_c$ . The quark masses used are  $m_{ud} = 0.1T_c$  and  $m_s = T_c$ . Taken from ref. [24].

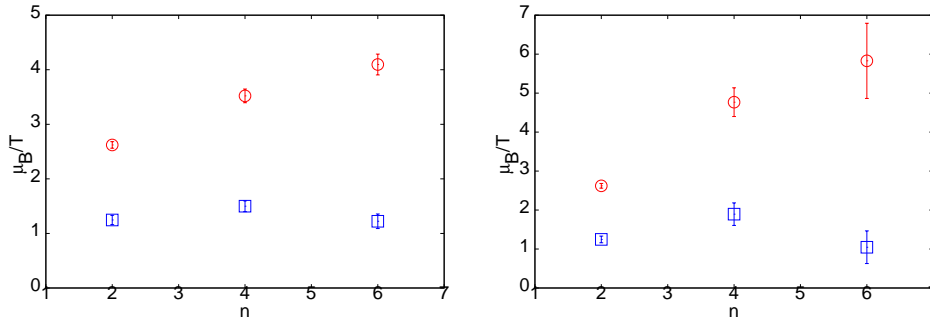


**Figure 7.** Radii of convergence  $\rho_n$  (left) and  $r_n$  (right) as a function of the order of the expansion at  $T = 0.95T_c$  on a  $4 \times 8^3$  lattice (circles) and a  $4 \times 24^3$  lattice (boxes). Taken from ref. [21].

such excitation. Such a picture is tantalizingly close to the canonical expectations of a transition from hadrons to quarks.

### 3.2 The critical point

Using both the definitions the radius of convergence in §3 for the terms up to 8th order in  $\mu$  in pressure (6th order in baryon number susceptibility), one obtains successively better estimates order by order. This can be done on each spatial volume, leading to a study of the volume dependence of the radius of convergence. Figure 7 shows the results for both  $\rho_n$  and  $r_n$  on the smallest ( $8^3$ ) and largest ( $24^3$ ) lattice.

Our results on the smaller lattice are consistent with the earlier estimate using re-weighting method. We observe strong finite size effects around  $N_s m_\pi \sim 6$  but our results on the largest lattice suggest a good stability with respect to an increase in the order of the expansion. Extrapolation in  $n$  leads to the following estimate

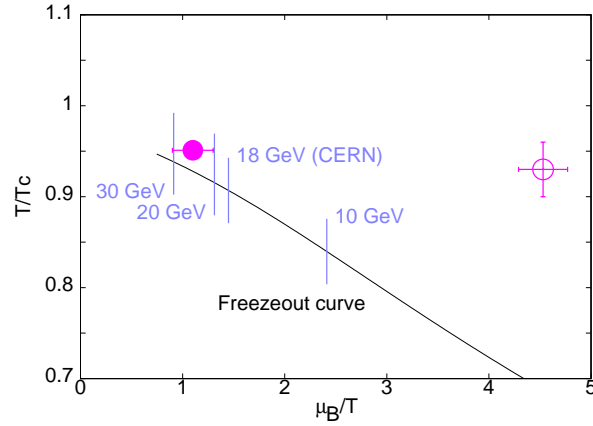


**Figure 8.** QCD phase diagram and the freeze-out curve superimposed. The filled and open circles denote our estimate [21] and an earlier estimate [19] of the critical point for nearly the same quark mass. A scale of the CM energy per nucleon,  $\sqrt{S}$ , has been marked on the freeze-out curve.

for the critical point:  $\mu^E/T^E = 1.1 \pm 0.2$  at  $T^E = 0.95T_c$ . Similar estimate has also been obtained recently for the re-weighting method, although the quark mass used (and hence the mass of the pion) was smaller in that case [27]. Another attempt to look [28] for the critical point using terms only up to 6th order did not find any critical point but they used much larger quark masses ( $m_\pi/m_\rho \sim 0.7$ ).

#### 4. Summary

Lattice QCD predicts new states of strongly interacting matter and is able to shed light on the properties of the quark-gluon plasma phase. One of the major developments of the recent past in lattice QCD is the firming up of the QCD phase diagram in  $\mu$ - $T$  plane on small  $N_t$ . Different fermions and different methods of simulations for nonzero  $\mu$ , all lead to a good agreement on the qualitative as well as the quantitative aspects. All estimates of  $T_c$ , and  $(T^E, \mu^E)$  are mutually consistent when compared with the right quark masses and in the thermodynamic limit. Our estimate for the critical point is  $\mu_B/T \sim 1$ – $2$ , as shown in figure 8. Also shown in the figure is a freeze-out curve [29], converted to a value of  $T_c$  appropriate to our computation. Such a curve results from the analysis of the heavy-ion data on particle yields. The required collision energy to reach the appropriate point are marked in the figure, which indicate the exciting possibility of discovering the critical point in a low-energy RHIC run in the near future.

Various physical quantities have been obtained in the continuum limit in the quenched approximation to QCD. These include the equation of state, the specific heat, the speed of sound in the neighbourhood of  $T_c$  and the quark number susceptibilities. While the former are needed in hydrodynamical analysis of the particle spectra, and the resultant collective flow, the latter (QNS) are directly relevant to

the physics of quark-gluon plasma signals at RHIC. The quenched lattice QCD estimate of Wróblewski parameter,  $\lambda_s$ , which is a measure of strangeness production in heavy-ion collision experiments, has been known to be in excellent agreement with the RHIC and SPS results.

Major efforts are on to extend these results to full QCD. Many features seem to change very little, although major change in the form of the order of the phase transition leads to quantitative differences near  $T_c$ . Interestingly, the robust Wróblewski parameter also does not change quantitatively near  $T_c$ , although one still needs more precise results and that too for realistic pion and kaon masses. Our results on baryon number-strangeness and electric charge-strangeness correlations suggest (i) a rapid change in going through the transition in full ( $N_f = 2$ ) QCD and (ii) the quark-gluon plasma to have quark-like excitations even close to  $T_c$ .

The heavy-ion data from CERN and BNL have provided us a lot of surprises, and will continue to do so in future. Lattice QCD has played an important part in understanding some of these, and clearly a lot more work is ahead both in the form of better precision as well as new ideas for experimentally measurable lattice predictions.

## References

- [1] F Wilczek, hep-ph/0512187
- [2] A Ali Khan *et al*, *Phys. Rev.* **D63**, 034502 (2001)
- [3] F Karsch, E Laermann and A Peikert, *Nucl. Phys.* **B605**, 579 (2001)
- [4] R V Gavai and S Gupta, *Phys. Rev.* **D65**, 094515 (2002); **D67**, 034501 (2003)
- [5] For a review, see e.g., R V Gavai, *Pramana – J. Phys.* **61**, 889 (2003)
- [6] C Bernard *et al*, PoS LAT2005, 156 (2005)
- [7] Y Aoki, Z Fodor, S D Katz and K K Szabo, *J. High Energy Phys.* **0601**, 089 (2006)
- [8] R V Gavai, S Gupta and S Mukherjee, *Phys. Rev.* **D71**, 074013 (2005)
- [9] R V Gavai, S Gupta and S Mukherjee, hep-lat/0506015
- [10] S S Gubser, I R Klebanov and A A Tseytlin, *Nucl. Phys.* **B534**, 202 (1998)
- [11] J-Y Ollitrault, *Pramana – J. Phys.* **67**(5), 899 (2006)
- [12] D Teaney, *Phys. Rev.* **C68**, 034913 (2003)
- [13] A Nakamura and S Sakai, *Phys. Rev. Lett.* **94**, 072305 (2005)
- [14] For a review, see e.g., R V Gavai, *Pramana – J. Phys.* **55**, 125 (2000)
- [15] NA50 Collaboration: G Borges, hep-lat/0505065  
PHENIX Collaboration: H Buesching, in *Proceedings of ‘Quark Matter 2005’*, *Nucl. Phys.* **A774**, 103 (2006)
- [16] S Datta *et al*, *Phys. Rev.* **D69**, 094507 (2004)
- [17] M Asakawa and T Hatsuda, *Phys. Rev. Lett.* **92**, 012001 (2004)  
T Umeda and H Matsufuru, hep-lat/0501002
- [18] S Datta *et al*, hep-lat/0409147
- [19] Z Fodor and S D Katz, *J. High Energy Phys.* **0203**, 014 (2002)
- [20] C R Allton *et al*, *Phys. Rev.* **D66**, 074507 (2002)  
Ph de Forcrand and O Philipsen, *Nucl. Phys.* **B642**, 290 (2002)  
M D’Elia and M P Lombardo, *Phys. Rev.* **D67**, 014505 (2003)  
R V Gavai and S Gupta, *Phys. Rev.* **D68**, 034506 (2003)
- [21] R V Gavai and S Gupta, *Phys. Rev.* **D71**, 114014 (2005)
- [22] S Gottlieb *et al*, *Phys. Rev. Lett.* **59**, 1513 (1987)

*Rajiv V Gvai*

- [23] R V Gvai and S Gupta, *Phys. Rev.* **D64**, 074506 (2001)  
R V Gvai, S Gupta and P Majumdar, *Phys. Rev.* **D65**, 054506 (2002)
- [24] R V Gvai and S Gupta, *Phys. Rev.* **D73**, 014004 (2006)
- [25] V Koch, A Majumder and J Randrup, *Phys. Rev. Lett.* **95**, 182301 (2005)
- [26] E V Shuryak and I Zahed, *Phys. Rev.* **C70**, 021901 (2004)
- [27] Z Fodor and S Katz, *J. High Energy Phys.* **0404**, 050 (2004)
- [28] C R Allton *et al*, *Phys. Rev.* **D71**, 054508 (2005)
- [29] J Cleymans, private communication